Turning Control for Quadruped Robots in Trotting on Irregular Terrain

Jeong Hoon Lee[1] and Jong Hyeon Park[2]

Abstract— **This paper proposes that a quadruped robot turns with an accurate turning radius through natural motion even if irregular terrain exists at the turning location. For a accurate and stable turning motion, two distinctive methods are proposed. First, the robot imitates a turning motion of animals such as a horse and a dog with their spine. To implement this, a scheme that is similar to a steering system of four-wheel-driven vehicle (4WS) at a low speed. Second, variable impedance control is used in passing an irregular terrain during the turning and maintaining a stable posture control. At the posture control, geometrical compensation scheme is additionally used for more accurate and sensitive control. Despite using these control methods, errors occur between desired turning radius and actual turning radius. In this paper, the errors are appropriately compensated in two steps. First of all, the errors are compensated by changing the stride and the directions of the axes of rotation of the feet motion when the errors are small. But, if the errors grow larger than a threshold, they is compensated by moving the feet in the lateral direction. The effectiveness of the proposed control schemes was verified in computer simulations.**

I. Introduction

Animals such as a horse and a dog turn everywhere and every time, and it consists of complicated movement of bones and muscles. Animal's turning is not calculative but instinctive, and very natural. Quadruped robots are difficult to turn naturally like an animal because the robot's legs consist of simple combinations of actuators and links [1]. Therefore, a comprehension of animal locomotion is preferentially required for the robot turning accurately and naturally.

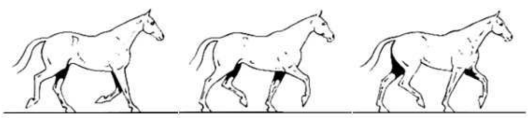

Fig. 1. Trotting of a horse

A horse and a dog have locomotion such as walk, trot, canter, gallop, and these locomotion are performed by natural transition of motion depending on various situations and environments [2]. Especially, the trot used in this study is locomotion which moves simultaneously diagonal to legs such as a left fore leg and a right hind leg. Due to this foot step type, the trot has the best energy efficiency in comparison with the other locomotion [3]–[5].

Also, an appropriate foot trajectory needs for the robot to trot stably, so an ellipsoidal trajectory is used [6], [7]. The ellipsoidal trajectory was made through observation of animal locomotion. Therefore, it comes naturally to not only a transformation of the trajectory but generation of a periodic motion. By the transformation and the periodic motion, the robot can turn. They are represented dynamic equations matching a operation type of differential system and a steering system of vehicle.

But, because it is impossible to express perfectly the robot locomotion by kinetics and kinematics, many assumptions and linearization need. Therefore, it is important to compensate appropriately large and small errors occurred in this process. To compensate the errors, basically PID control is used, and also impedance control is used to cope with impact generated during the locomotion and unstable environment such as uneven and slippery surfaces [7]–[9].

But, impedance control is difficult to compensate large disturbance because it exists a range of parameters coping with size of disturbances. Therefore, another control method needs to control roll and pitch angle generated excessively by disturbances. To control the roll and the pitch angle, the robot uses geometrically computed values resulting from slanting of the robot body, and it is implemented by changing height of contacted legs on the surface [10], [11].

In this paper, an elaborate control scheme for a quadruped robot to turn with an accurate turning radius even on a irregular terrain is proposed. In this scheme, the robot imitates turning of animals with their spine, and variable impedance control is used. Also, a geometrical method is used for posture control additionally. Errors occurred between desired turning radius and actual turning radius during the turning are compensated through a stepwise approach. When errors are small, they are compensated by changing the stride and the direction of the axis of rotation for the elliptical motion of each feet. But, if the errors grow larger than a threshold, the foot trajectory is compensated by moving the feet in the lateral direction. The stability of the turning and the performance of the control scheme were verified in computer simulations.

II. Generation of Foot Trajectory for Turning

Animal's turning consists of diverse and complicated mechanisms. To turn, quadrupeds such as a horse and a dog lean their body by taking down shoulder in the turning direction, and they control a velocity by changing the stride between outside legs and inside legs. Also, while Animals draw the outside legs, they stretch the inside legs. These behaviors are observed more clearly at high speed locomotion such as dog race. A noteworthy part of this animal's turning mechanism is similar to operational principle of a differential

[1]J. Choo is with Dept. of Mechanical Engineering, Hanyang University, Seoul, 133-791, Korea. `ljhdragon@naver.com`

[2]J. H. Park with with School of Mechanical Engineering, Hanyang University, Seoul, Korea. `jongpark@hanyang.ac.kr`

ISBN: 978-1-61804-242-2

system and a steering system of four-wheel drive (4WS). Therefore, a basic control methods for the turning is methods for changing the stride between outside legs and inside legs as the differential system and rotating the trajectory on z-axis as the steering system.

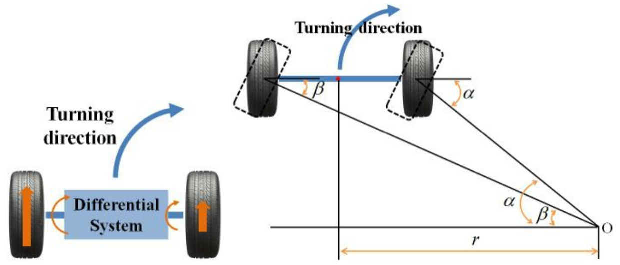

(a) Differential system (b) Steering system : Acherman-Jantoud type

Fig. 2. Differential system and steering system in a car

A. Half-Ellipsoidal Foot Trajectory

In this paper, a desired foot trajectory of the robot take a form of half-ellipsoid. The half-ellipsoidal trajectory is very similar to animal's one, and the advantages is as follows.

1. It is rhythmical and continuous.
2. Transformation of the trajectory is easy.
3. The robot can move forward without changing the body height in comparison with a whole ellipsoidal trajectory.

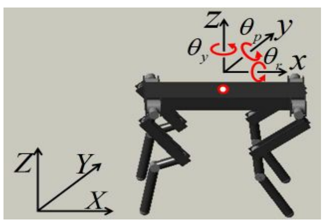

(a) Robot model : RPY angles of yaw ϕ_y, pitch ϕ_p, roll ϕ_r

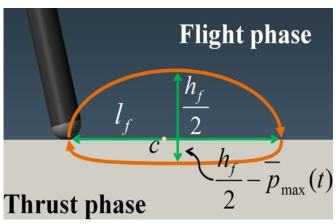

(b) Half-ellipsoidal trajectory

Fig. 3. Coordinate systems, body angles and ellipsoidal trajectory

The foot trajectory is generated with respect to the robot body, and each direction of axis(x-y-z) and RPY angles is same as shown in Fig. 3(a). The equations of the half-ellipsoid are

$$\bar{x}(t) = \frac{l_{\rm f}}{2}\sin\left(\frac{2\pi}{T}t + \theta_{\rm i}\right) + c_1, \qquad \text{for } 0 \le t \le T \quad (1)$$

$$\bar{y}(t) = c_2, \qquad \text{for } 0 \le t \le T \quad (2)$$

$$\bar{z}(t) = \frac{h_{\rm f}}{2}\cos\left(\frac{2\pi}{T}t + \theta_{\rm i}\right) + \bar{p}(t) + c_3, \qquad \text{for } 0 \le t \le T \quad (3)$$

where $l_{\rm f}$ is the stride, $h_{\rm f}$ is the maximum foot height, T is the one step period, $\theta_{\rm i}$ is the initial phase, c_1, c_2 and c_3 are center points of the ellipsoid, and $\bar{p}(t)$ is a 3rd order polynomial equation. Especially, $\bar{p}(t)$ is used to generate the half-ellipsoid and prevent non-differentiable point. This can avoid a occurring problem when impedance control module is composed.

B. Rotation of Foot Trajectory

A car steering system is rotated wheels, and it is similar to being rotated the foot trajectory of the robot on z-axis. The trot is locomotion moving the four legs simultaneously. Therefore, the trot is associated with movement of 4WS. Especially, 4WS has a feature called a opposite direction at low speed which has a opposite phase of fore wheels and rear wheels. Also, the opposite direction is very similar to turning of animal with the spine, so it is suitable for applying to turning of the robot without the spine as shown in Fig. 4. The painted rectangles of Fig. 4(c) are a range of the stride.

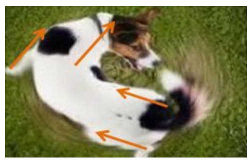

(a) Animal with the spine

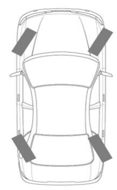

(b) 4WS : low speed

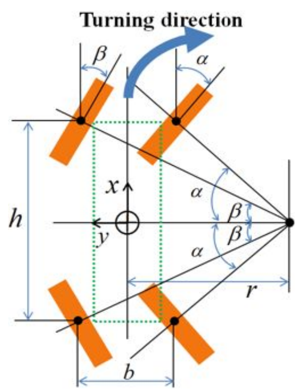

(c) Turning of robot

Fig. 4. Turning of robot : Differential system of 4WS

The circle drawn by tracing the foot trajectory is that the inner circle is smaller than the outer circle. It is associated with the fundamental steering system, Ackerman-Jantoud type, and the equations are

$$\alpha = \tan^{-1}\left(\frac{h}{2r-b}\right) \quad \text{and} \quad \beta = \tan^{-1}\left(\frac{h}{2r+b}\right),$$

where h and b are the length and the width of the robot body, respectively, r is the turning radius, and α and β are the inner and outer steering angles, respectively. Eventually, the trajectory rotates α and β on z-axis as shown in Fig. 4(c), and rotation matrix is used for the rotation.

$$\begin{bmatrix} \bar{x}_{\rm r}(t) \\ \bar{y}_{\rm r}(t) \\ \bar{z}_{\rm r}(t) \end{bmatrix} = \begin{bmatrix} \cos\phi_{\alpha\beta} & -\sin\phi_{\alpha\beta} & 0 \\ \sin\phi_{\alpha\beta} & \cos\phi_{\alpha\beta} & 0 \\ 0 & 0 & 0 \end{bmatrix} \begin{bmatrix} \bar{x}(t) \\ \bar{y}(t) \\ \bar{z}(t) \end{bmatrix}, \quad (4)$$

where $\phi_{\alpha\beta}$ means α or β according to location of legs. Therefore, $\bar{x}_{\rm r}(t)$, $\bar{y}_{\rm r}(t)$ and $\bar{z}_{\rm r}(t)$ are the foot trajectory during the turning.

ISBN: 978-1-61804-242-2

C. Transformation of Foot Trajectory

As shown in Fig. 4(c), the angular velocity of the robot body rotating at given turning radius is the same as the outer and inner legs'. But, the outer and inner legs differ in the linear velocity. Therefore, difference between the linear velocity of inner legs and the linear velocity of outer legs is calculated using this correlation.

$$w = \frac{v + v_{\mathrm{o}}}{r + \frac{b}{2}} = \frac{v + v_{\mathrm{i}}}{r - \frac{b}{2}} = \frac{v}{r} \ , \tag{5}$$

$$v_{\mathrm{o}} = -v_{\mathrm{i}} = \frac{vb}{2r} \ , \tag{6}$$

where w is an angular velocity of the robot body, v is a linear velocity of the robot body, and v_o and v_i are variation of the linear velocity of inner and outer legs, respectively. Therefore, $v + v_{\mathrm{o}}$ and $v + v_{\mathrm{i}}$ are linear velocitys of outer and inner legs, respectively.

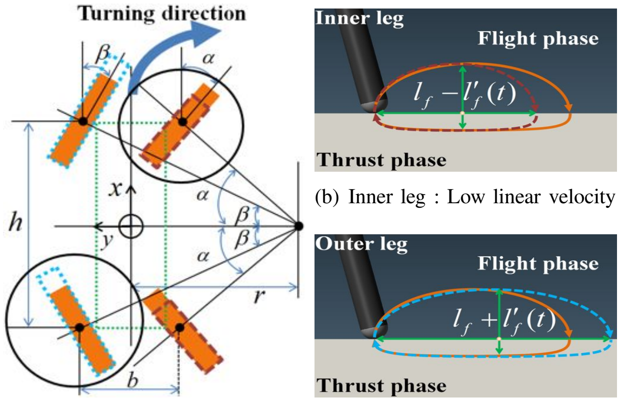

(a) Differential system (b) Inner leg : Low linear velocity (c) Outer leg : High linear velocity

Fig. 5. Turning of robot : Differential system of 4WS

Changing the rotating velocity of inner and outer wheels by the differential gear is similar to changing the stride as shown dotted lines in Fig. 5. To perform this, a transformation of the trajectory needs. The half-ellipsoidal trajectory can transform easily, but the length of the trajectory, the stride dose not. If the transformation of the stride is attempted forcedly, continuity of the trajectory is difficult to be guaranteed. Therefore, a method for natural transformation of the trajectory needs, so this paper proposes to make the stride into a function over time.

$$\bar{x}(t) = \frac{l_{\mathrm{f}} \pm \bar{l}_{\mathrm{f}}(t)}{2} \sin\left(\frac{2\pi}{T}t + \theta_{\mathrm{i}}\right) + c_1, \qquad \text{for } 0 \le t \le T \tag{7}$$

which is a form that $\bar{l}_{\mathrm{f}}(t)$ is added to (1). $\bar{l}_{\mathrm{f}}(t)$ is 3rd polynomial equation ranging in size from 0 to v_{o}, and a plus sign and a minus sign mean the outer foot trajectory and the inner foot trajectory, respectively. Of course, (7) is also rotated by (4).

D. Banked Roll Angle of Robot Body

When a car turning a circular track at given speed is no slip in any direction, equations that no friction between the road and wheels exists are

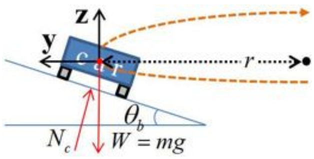

$$N_{\mathrm{c}} \sin\theta_{\mathrm{b}} = m\frac{v^2}{r}, \tag{8}$$

$$N_{\mathrm{c}} \cos\theta_{\mathrm{b}} - mg = 0, \tag{9}$$

Fig. 6. Banked roll of a car

where N_{c} is reaction force, θ_{b} is a banked angle, r is a turning radius and v is a linear velocity of the car. θ_{b} is found by solving simultaneous equations (8) and (9).

$$\theta_{\mathrm{b}} = \tan^{-1}\left(\frac{v^2}{gr}\right). \tag{10}$$

Angle θ_{b} can be also applied to the banked roll angle of the robot body in turning as shown in Fig. 7.

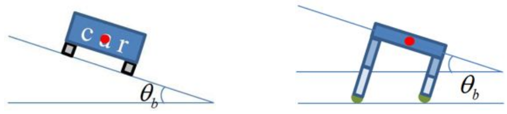

(a) Car (b) Quadruped robot

Fig. 7. Banked roll : Car and Quadruped robot

When angle θ_{b} is applied to the robot, r and v are the given turning radius and the stride per second, respectively. Eventually, the robot leans the body at θ_{b} during the turning.

III. Impedance Control

Impedance control is effective, especially for reducing the disturbance. The irregular terrain is a kind of disturbance. Therefore, impedance control plays important roles in turning on irregular terrain.

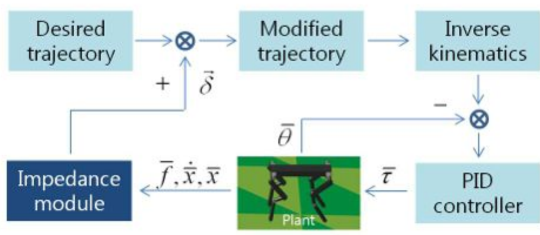

Fig. 8. Impedance control block diagram

As shown in Fig. 8, input of the impedance module is force $\bar{f}$, then output is position offset $\bar{\delta}$. Therefore, this impedance control can be defined admittance control.

$$\ddot{\bar{\delta}} = \frac{1}{M}[\bar{f} - B\dot{\bar{\delta}} - K\bar{\delta}], \tag{11}$$

where M, B and K are parameters of impedance module. M is the mass, B is the critical damping ratio $B = 2\sqrt{MK}$ and

ISBN: 978-1-61804-242-2

K is the stiffness. The critical damping ratio can decrease most rapidly effects of impact (i.e., overshoot) changing the desired trajectory. After integrating $\ddot{\bar{\delta}}$ of (11) twice, $\bar{\delta}$ is added to the desired trajectory.

IV. Control for the Robot Posture

Although impedance control is used to locomotion of the robot, the robot is difficult to trot stably in all environment. Because there is a limit to the parameter of impedance control which can cope with the disturbance. Therefore, if the robot encounters disturbance such as irregular terrain during the turning, the roll angle ϕ_{r} and the pitch angle ϕ_p of the robot body increase rapidly. So, the body angles must be controlled for the robot turning stably. In trotting, ϕ_{r} and ϕ_p affect each other. But, if correlation of the angles is not figure out, simultaneously compensating the angles rather make the posture unstably. Therefore, method for compensating the excessive ϕ_{r} that generally has larger range of variation than ϕ_p is selected. For example, if the sizes of rolling and pitching of the robot body are almost identical (i.e., in stable trotting), ϕ_p is always smaller than ϕ_{r}. Because the robot body is rectangle that the length h is taller than the width b as shown in Fig. 4(c).

A. Geometrical Compensation of Roll Angle

The most common method for compensating the excessive ϕ_{r} is a geometrical method as shown in Fig. 9.

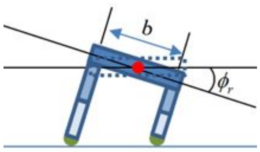

(a) Front view of the robot

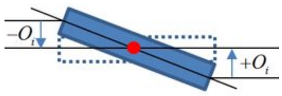

(b) Robot body

Fig. 9. Geometrical compensation : O_{i}

The equation of the size (i.e., O_{i}) is

$$O_{\mathrm{i}} = \frac{b}{2}\sin(\phi_{\mathrm{r}} - \theta_{\mathrm{b}}), \tag{12}$$

where O_{i} is O of i_{th} state. i_{th} state means order of sampled roll angles with sample time. θ_{b} is a banked roll angle. Therefore, unstability of the posture can is modified by adding O_{i} to (3).

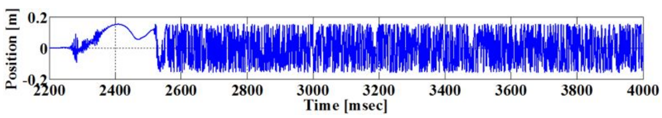

(a) O_{i} in sample time, 0.001sec

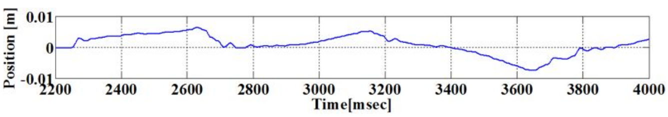

(b) O_{i} in sample time, 0.02sec

Fig. 10. Comparison of O_{i} with sample time

But, O_{i} is generated very unstable values as shown in Fig. 10(a) because the robot works in very short sample time, 0.001 sec during the simulation.

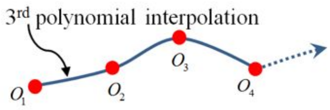

Fig. 11. 3rd polynomial interpolation of O_{i}

Therefore, the robot is required appropriate sample time which can reflect the accurate body angles not having a short oscillation cycle. In this paper, the determined sample time of ϕ_{r} is 0.02 sec, and because of altered sample time, interpolation is required as shown in Fig. 11.

B. Variable Impedance Control And Geometrical Compensation

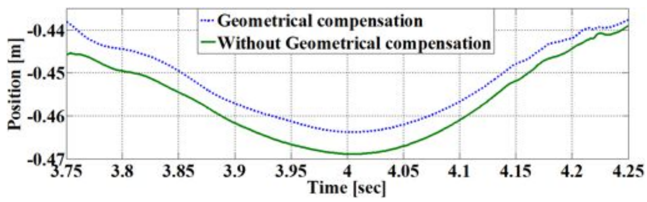

Fig. 12. Foot trajectory compensated by impedance control on z-axis

But, method for compensating the excessive ϕ_{r} by moving the center of the foot trajectory is not suitable for the locomotion using impedance control. Because, by impedance control, O_{i} is also compensated. The dotted line of Fig. 12 is made by O_{i}, 0.01 m, but generally the trajectory on z-axis is compensated by about 0.005 m. In other words, the error is compensated only half. To solve this problem, variable impedance control that can control the excessive ϕ_{r} changing impedance parameter in real time is used in form of servo control as shown in Fig. 13.

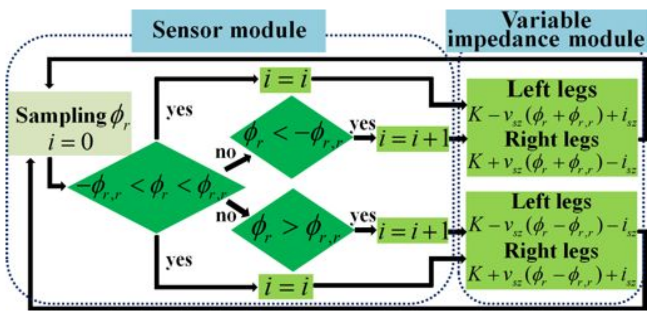

Fig. 13. Variable impedance control: $\phi_{\mathrm{r,r}}$ is reference roll angle.

$$\ddot{\bar{\delta}} = \frac{1}{M_{\mathrm{i}}}[\bar{f} - B_{\mathrm{i}}\dot{\bar{\delta}} - K_{\mathrm{i}}\bar{\delta}], \tag{13}$$

where M_{i}, K_{i} and B_{i} are the impedance parameters of i_{th} state. Especially, K_{i} of (13) means $K \pm v_{\mathrm{sz}}(\phi_{\mathrm{r}} + \phi_{\mathrm{r,r}}) \mp i_{\mathrm{sz}}$ and $K \pm v_{\mathrm{sz}}(\phi_{\mathrm{r}} + \phi_{\mathrm{r,r}}) \pm i_{\mathrm{sz}}$ of Fig. 13, and it is a linear

ISBN: 978-1-61804-242-2

function of stiffness that variable is ϕ_{r}. i_{sz} and v_{sz} of the linear function are a y-intercept and a slope, respectively. B_{i} is the critical damping ratio. Also, After integrating $\ddot{\bar{\delta}}$ of (13) twice, position offset $\bar{\delta}$ is added to the desired trajectory as shown in Fig. 8. But, such servo control is difficulty to control the excessive ϕ_{r} sensitively and accurately. Therefore, additionally the geometrical method is used to make up for this fault. In other words, the size of O_{i} decreases by multiplying the gain, and The decreased O_{i} can control ϕ_{r} sensitively and accurately.

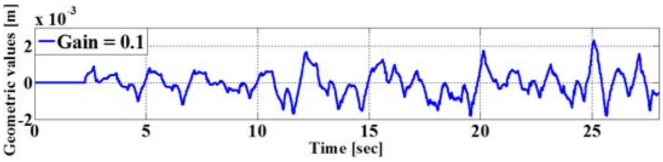

Fig. 14. O_{i} multiplied by gain

This is similar to method compensating error using PID controller. Variable impedance control is used to main control method for compensating the excessive ϕ_{r} like using proportional control of PID controller, and the occurred steady state error and slowed speed of response is compensated by the geometrical method like using integral control and differential control of PID controller.

C. Compensation of Turning Error

Although introduced methods such as transformation and rotation of the trajectory, posture control, etc. is used appropriately, still the turning error exists between desired turning radius and actual turning radius.

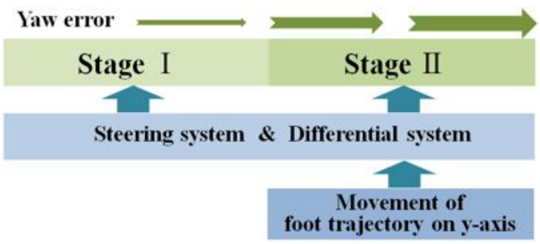

Fig. 15. Stepwise compensation method

Therefore, the error needs to be compensated appropriately, so a stepwise approach is used as shown in Fig. 15.

At first stage that the error is smaller than the threshold, the error is compensated by differential system and steering system. In other words, the variation of the stride and the rotation of the foot trajectory are added to (7) and (4), respectively during one step period. At the second stage that the error grows larger than the threshold, the foot trajectory on y-axis is moved as shown in Fig. 16(b). The equation of the second stage is

$$\bar{y}(t) = c_2 + \bar{m}(t), \qquad \text{for } 0 \leq t \leq T \qquad (14)$$

which is a form that $\bar{m}(t)_{\mathrm{f}}$ is added to (2). $\bar{m}(t)_{\mathrm{f}}$ is 3rd polynomial equation, and the size (i.e., $r_{\mathrm{a}} - r_{\mathrm{d}}$ as shown in Fig. 16(b)) is determined by considering workspace of the robot.

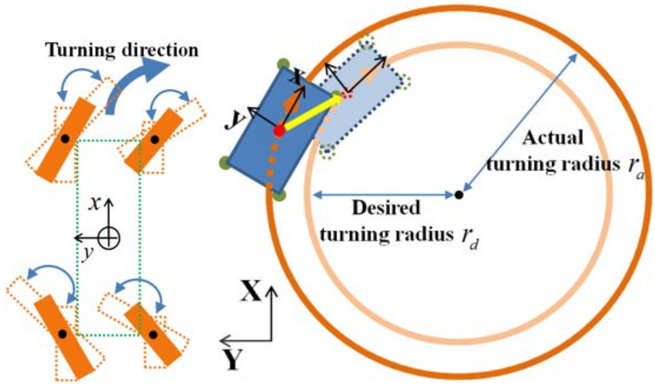

(a) Differential system and steering system (b) Movement of trajectory on y-axis

Fig. 16. Compensation of turning error

V. Simulation

As shown in Fig. 3(a), the robot model simplifies a hardware model HUNTER (Hanyang UNiversity TEtrapod Robot) developed by Hanyang University. HUNTER is 0.5 m tall and 0.35 m wide. Its head-to-tail length is 0.6 m. It weights about 24 kg.

Fig. 17. Irregular terrain model

The simulation is processed by using Mathworks's Matlab and Functionbay's RecurDyn. Spring coefficient and damping coefficient between ground and robot foot are each 2000 kN/m and 1.0 kN·s/m. Dynamic friction coefficient and static friction coefficient are 0.6 and 0.9, respectively. l_{f} and h_{f} are 0.100 m and 0.080 m, respectively, the one step period is 1 sec and the turning radius is 1.5 m. As shown in Fig. 17, irregularities of the terrain are 0.017 m, 0.02 m, 0.015 m and 0.017 m in a clockwise direction, respectively.

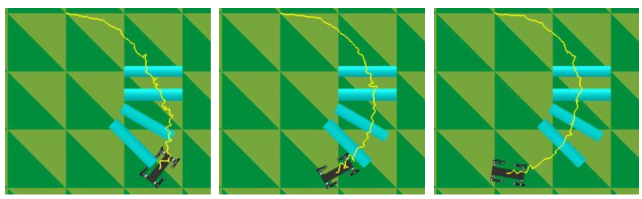

(a) Fixed impedance (b) Variable impedance (c) Variable impedance with geometrical method

Fig. 18. Top view of the robot during the turning

Fig. 18 shows results depending on each condition. When fixed impedance control is used, the robot escapes the route.

In the case of Fig. 18(b) using variable impedance control, the distance traveled is shorter than in the case of Fig. 18(c) because the robot body excessively sways by the rolling. Also, Fig. 19 shows that the robustness and the stability of the proposed posture control is verified. And, as shown in Fig. 20, variable impedance control is performed appropriately.

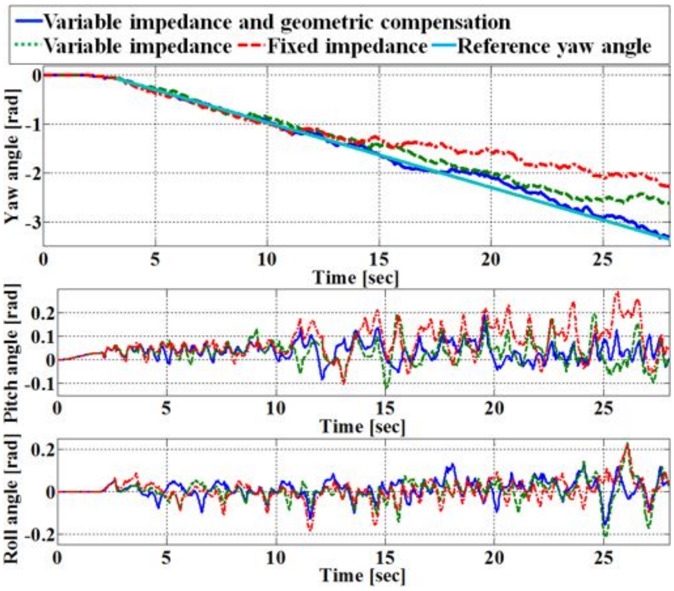

Fig. 19. Body angles (ϕ_r, ϕ_p, ϕ_y) on each condition

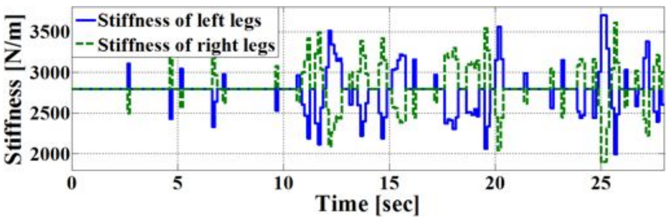

Fig. 20. Variable impedance control for robot posture control

Figs. 21 and 22 show that the generation of the foot trajectory during the turning and the stepwise compensation of the turning error is operated appropriately. In other words, Fig. 21 is the foot trajectory generated by the differential system, the steering system and the posture control, and Fig. 22 is the application result of (14).

VI. Conclusion

In this paper, various methods for the quadruped robot turning accurately on irregular terrain is proposed. Basically the robot imitates the operation type of differential system and steering system of 4WS at low speed. Especially, the steering system of 4WS at low speed, an opposite direction is represented as animal's turning with the spine. Also, variable impedance control and geometrical compensation is simultaneously used to eliminate unstability of the posture generated during the robot turning. The turning error existing between desired turning radius and actual turning radius is

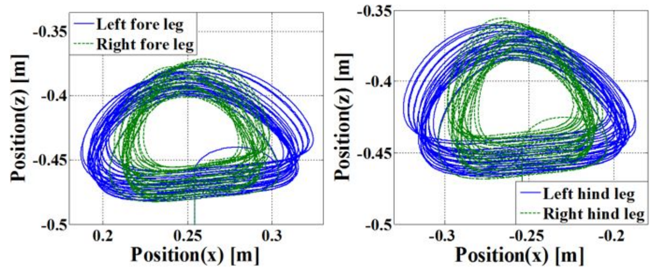

(a) Trajectorys of fore legs (b) Trajectorys of hind legs

Fig. 21. Trace of foot trajectory

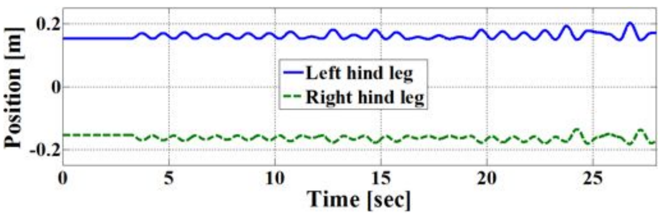

Fig. 22. Movement of foot trajectory on y-axis

compensated by stepwise approach. The variation of the stride and the rotation of the foot trajectory is used at the first stage and the method moving the center of the foot trajectory on the y-axis is used at the second stage. The proposed control methods have shown even better stability and performance than the control groups.

References

[1] L. R. Palmer III and D. E. Orin, "Intelligent control of high-speed turning in a quadruped," *Journal of Intelligent and Robotic Systems*, vol. 58, no. 1, pp. 47–68, 2010.

[2] R. M. Alexander, *Principles of animal locomotion*. Princeton University Press, 2003.

[3] J. Glower and U. Ozguner, "Control of a quadruped trot," in *Proceedings of IEEE International Conference on Robotics and Automation*, 1986, pp. 1496–1501.

[4] R. Kurazume, S. Hirose, and K. Yoneda, "Feedforward and feedback dynamic trot gait control for a quadruped walking vehicle," in *Proceedings of IEEE International Conference on Robotics and Automation*, 2001, pp. 3172–3180.

[5] M. H. Raibert, "Trotting, pacing and bounding by a quadruped robot," *Journal of biomechanics*, vol. 23, pp. 79–98, 1990.

[6] K. Y. Kim, O. Kwon, J. S. Yeon, and J. H. Park, "Elliptic trajectory generation for galloping quadruped robots," in *Proceedings of IEEE International Conference on Robotics and Biomimetics*, 2006, pp. 103–108.

[7] J. H. Lee and J. H. Park, "Control for quadruped robots in trotting on horizontal and slanted surfaces," in *Control Conference (ASCC), 2013 9th Asian*. IEEE, 2013, pp. 1–6.

[8] J. H. Park, "Impedance control for biped robot locomotion," *IEEE Transactions on Automatic Control*, vol. 17, no. 6, pp. 870–882, 2001.

[9] R. Ikeura and H. Inooka, "Variable impedance control of a robot for cooperation with a human," in *Robotics and Automation, 1995. Proceedings., 1995 IEEE International Conference on*, vol. 3. IEEE, 1995, pp. 3097–3102.

[10] M. Raibert, K. Blankespoor, G. Nelson, R. Playter *et al.*, "Bigdog, the rough-terrain quadruped robot," in *Proceedings of the 17th World Congress*, 2008, pp. 10 823–10 825.

[11] H. Kimura, Y. Fukuoka, and A. H. Cohen, "Adaptive dynamic walking of a quadruped robot on natural ground based on biological concepts," *International Journal of Robotics Research*, vol. 26, no. 5, pp. 475–490, May 2007.